On the Microscopic Structure of Neat Linear Alkylamine Liquids: an x-ray Scattering and Computer Simulation Study

Martina Požar, Lena Friedrich, Tristan Millet, Michael Paulus, Christian Sternemann, Aurélien Perera

On the Microscopic Structure of Neat Linear Alkylamine Liquids: an x-ray Scattering and Computer Simulation Study

Martina Požar[1], Lena Friedrich[2], Tristan Millet[3]
Michael Paulus[2], Christian Sternemann[2*]and Aurélien Perera[3 †]

October 7, 2024

[1]Faculty of Science, University of Split, Ruđera Boškovića 33, 21000 Split, Croatia

[2]Fakultät Physik/DELTA, Technische Universität Dortmund, D-44221 Dortmund, Germany

[3]Laboratoire de Physique Théorique de la Matière Condensée (UMR CNRS 7600), Sorbonne Université, 4 Place Jussieu, F75252, Paris cedex 05, France.

Abstract

Linear amines, from propylamine up to nonylamine, are studied at ambient conditions by x-ray scattering and Molecular Dynamics simulations of various force field models. The major finding is that the pre-peak in alkylamines is of about one order of magnitude weaker than that in alkanols, hence suggesting much weaker hydrogen bonding induced clustering of the amine groups than for the hydroxyl groups. Computer simulation studies reveal that OPLS-UA model reproduces the pre-peak, but with larger amplitudes, while the GROMOS-UA and CHARMM-AA force fields show almost no pre-peak. Simulations of all models show the existence of hydrogen bonded clusters, equally confirmed by the prominent pre-peak of the structure factor between the nitrogen atoms. The hydrogen bond strength, as modeled by the Coulomb association in classical force field models, is about the same order of magnitude for both systems. Then, one may ask what is the origin of the weaker pre-peak in alkylamines? Simulation data reveals that the existence of the pre-peak is controlled through the cancellation of the positive contributions from the charged group correlations by the negative ones from the cross charged-uncharged correlations. The C2v symmetry of the amine head

*christian.sternemann@tu-dortmund.de
†aup@lptmc.jussieu.fr

group hinders clustering, which favours cross correlations with the tail atoms. This is opposite to alkanols where the symmetry of hydroxyl head group favours clustering and hinders cross correlations with the alkyl tail. This competition between charged and uncharged atomic groups appears as a general mechanism to explain the existence of scattering pre-peaks, including their position and amplitude.

1 Introduction

Several recent studies of alcohols have put forward the rich variety of hydrogen bonded hydroxyl group aggregates, both from x-ray scattering experiments[1–9] and computer simulations.[10–16] The latter studies have demonstrated the chain-like association patterns of the OH groups, witnessing plain and branched chains, as well as loops and lassos.[15,16] These studies have also highlighted the importance of the alkyl chains, which are not simply low energy inert components which follow the association tendencies of the high energy polar head groups, but they contribute entropically to reduced and condition the association of the hydroxyl heads. Since self-assembly and self-association are not only limited to hydrogen bonding between the OH groups, it is interesting to investigate whether other forms of associations are equally rich in patterns. The next in the list is the amine group NH2, which is somewhat reminiscent of the water OH2 geometry. Yet, it also reminds that, whereas water is the "mother" of the hydrogen bonding liquids,[17–23] interestingly enough, it lacks the demonstrative hydrogen bonding patterns that the alcohols show. Indeed, whereas alcohols demonstrate the existence of aggregates in the x-ray scattering through the pre-peak feature,[2,5,8,15] water has no such pre-peak, but a weak shoulder pattern.[24] This lack of aggregate signature is equally observed in cluster distributions calculated from computer simulations: all alcohols show an universal OH pentamer leading cluster pattern, while water has quite a featureless cluster distribution not very different from that of a standard Lennard-Jones liquid.

Interestingly, unlike alkanols, smaller alkylamines such as methylamine and ethylamine are not liquid in ambient conditions. This is already an indication that the hydrogen bonding between the amine groups alone is not able to stabilize a dense liquid, unlike the hydroxyl groups for very small alkyl chains. An indirect conclusion is that longer alkyl chains help stabilize the liquid state starting from proplylamine. This conclusion was not obvious from the previous studies of alkanols. Indeed, most short alkanes, such as methane to butane, are also not liquids in ambient conditions.[25] All this points to the essential role of the hydrophobic tails when combined with hydrogen bonding head groups.

Another interesting issue is that of the model representation of the molecular liquids when dealing with computer simulations. Several studies have highlighted the importance of studying various force field models.[15,16] For instance the scattering pre-peak shape for linear monools differs appreciably from one force field model to another. This is quite simply related to small differences in the geometrical packings of the various charged groups, which we call charge

ordering, which add up in the structure correlation functions and reflect upon the total scattering intensity, since the latter is a sum over all partial atom-atom structure factors.

Following our recent work on x-ray scattering and simulation study of alkanols,[15] we investigate amines, which show a quite weak x-ray scattering pre-peak. We are concerned with the microscopic reason for this property, particularly as revealed through pair correlation functions and associated structure factors. These two quantities although not directly available through experiments, contribute to the x-ray scattering, hence help explain its feature. However, they are accessible through simulation and are biased by the choice of force field models. We try to obtain explanations that are independent of this bias.

The literature is scarce when it comes to either experimental or simulations studies of the structure of liquid amines. The earliest work on x-ray diffraction appears to be that of Thosar[26] in 1938, who reports invariance of the main peaks positions for various amines. This feature is now trivially explained in terms of the van der Waals radii similarities between the carbon and nitrogen atoms. Excluding the previous work of some of the authors,[27] there are equally x-ray scattering experimental results on solid state amines.[28,29] As for the simulations, studies that feature the structuring in neat amines include that of Kusalik and coworkers,[30] Kosztolányi et al.[31] and Bauer and Patel.[32] The former two papers describe the structure in methylamine, while the latter paper of Bauer and Patel[32] features methylamine, ethylamine and propylamine. The group of Lachet did extensive work on force field development of primary, secondary and tertiary amines,[33,34] with subsequent investigations about the transport properties of amines[35] and gas solubility in amines.[36] There were also simulation studies about transport properties[37] and diffusion of amines[38] undertaken by other authors. However, the remainder of the literature of amine simulations has the overarching theme of industrial applications in the context of CO_2 capture[39–41] and the development and improvement of various materials.[42–44]

2 Technical considerations

2.1 Experimental setup

The wide-angle x-ray diffraction experiment was performed at beamline BL9 of the DELTA synchrotron radiation source (Dortmund, Germany).[45] Propylamine (99%) butylamine (99.5%), pentylamine (99%), hexylamine (99%), heptylamine (99%), octylamine ($\geq$ 99.5%) and nonylamine (MQ200) were purchased from Sigma-Aldrich and used without further treatment. The liquids were filled into borosilicate glass capillaries of 1.5 mm diameter prior to the measurements and capillaries were sealed. The incident photon energy was set to 20 keV which refers to a wavelength of 0.61992$\AA$ and the scattered intensity was measured using a MAR345 image plate scanner. The setup was calibrated with the diffraction image of a CeO_2 reference sample. In order to better assess the air scattering background because of the weak pre-peak signals, diffraction

data were taken with and without a He beam path placed behind the sample holder. The measured diffraction images were integrated using the program package Fit2D.[46] Finally the background due to scattering from air and the glass capillary was subtracted and the diffraction patterns were normalized by their integral in the momentum-transfer k range between 0.37 and 3 $\mathring{A}^{-1}$ to their calculated counterparts, i.e. the averaged integral value of all calculated diffraction intensities for a certain sample. Except for nonylamine, diffraction data in the k-range between 0.035 and 0.3 $\mathring{A}^{-1}$ has been measured independently at the small angle x-ray scattering beamline BL2 of DELTA using the setup as describe in Ref.[47] with an incident energy of 12 keV, i.e. a wavelength of 1.0332$\mathring{A}$. The calibration of the setup was performed with a silver behenate reference and the raw data were treated as discussed for the wide-angle x-ray scattering measurements. For representation, both data taken at BL9 and BL2 were merged using a scaling factor in the k-range were both sets overlap

2.2 Computer simulation and theoretical details

We performed molecular dynamics simulations of neat amines in the Gromacs program package.[48] In our previous work,[27,49] we chose the force field Gromos 53a6[50] for propylamine, courtesy of the Automated Topology Builder.[51] Due to our previous experiences with linear alcohols,[15] we examined different force fields: the CHARMM all-atom,[52–54] GROMOS 54a7 united-atom[55] (from butylamine to octylamine) and OPLS united-atom.[56,57]

PACKMOL[58] was used to create the initial configurations of 2048 molecules for all amines, which underwent energy minimization and equilibration for 4 ns. Production runs of 2 ns were performed, during which at least 2000 configurations were collected. The simulations were done in the NpT ensemble at ambient conditions, $T = 300$ K and $p = 1$ bar. The temperature was maintained with the v-rescale thermostat,[59] whereas the the Parrinello-Rahman barostat[60,61] was used to keep the pressure constant. The temperature algorithm had a time constant of 0.2 ps and the pressure algorithm was set at 2 ps.

The integration algorithm was leap-frog,[62] which had the time step of 2 fs. The short-range interactions were calculated within the 1.5 nm cut-off radius, while the long-range electrostatics were handled with the PME (Partial Mesh Ewald) method.[63] The LINCS algorithm[64] handled the constraints.

The scattering intensity was calculated via the Debye formula:[65,66]

$$I(k) = r_0^2 \rho \sum_{ij} f_i(k) f_j(k) S_{ij}(k) \tag{1}$$

where $\rho = N/V$ is the density (where N is the number of molecules in the volume V), the $f_i(k)$ functions are the form factor of atom i, and $r_0 = 2.8179 \cdot 10^{-13}$cm is the electronic radius. The total structure factor $S_{ij}(k)$ is defined as:[15]

$$S_{ij}(k) = w_{ij}(k) + \rho H_{ij}(k) \tag{2}$$

where $w_{ij}(k)$ the intra-molecular atom-atom structure factor, $H_{ij}(k)$ is related to the Fourier transform of the atom-atom intermolecular pair correlation function $g_{ij}(r)$

$$H_{ij}(k) = \int d\vec{r}\,[g_{ij}(r) - 1] \exp(i\vec{k} \cdot \vec{r}) \tag{3}$$

The pair correlation functions $g_{ij}(r)$ are calculated directly from the Gromacs trajectory files (using the gmx_g_rdf program), while the intra-molecular parts $w_{ij}(r)$ are calculated as described in Ref.[15] by sampling the mean atom-atom distance histograms within each molecules in several configurations.

3 About the very small scattering pre-peak in relation to the amine group clustering

3.1 X-ray scattering

Fig.1 shows a comparison of the x-ray scattering intensity $I(k)$ between the experimental data for all alkylamines (left panel) and the $I(k)$ calculated from different simulation models (right panel).

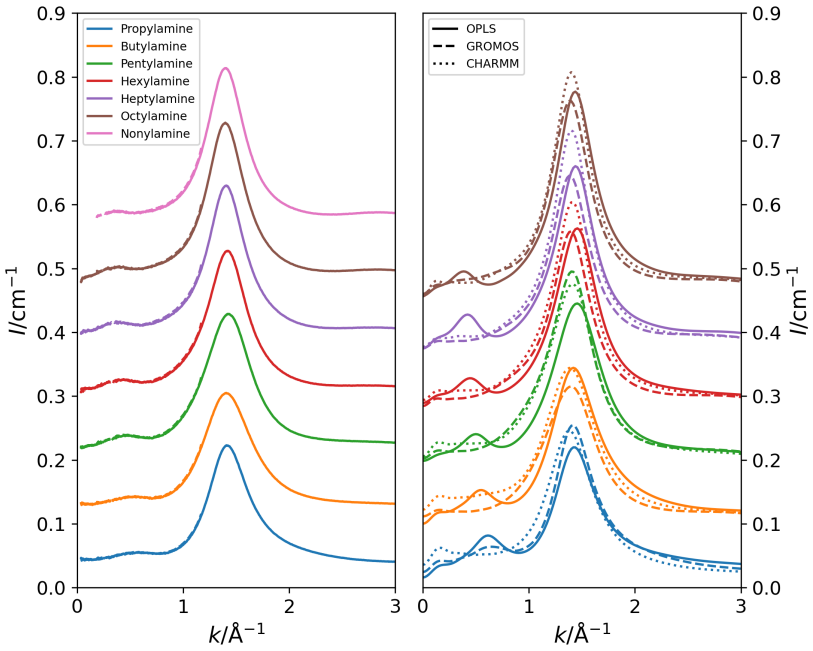

Figure 1: X-ray scattering intensities $I(k)$ for all alkylamines (each shifted by 0.1 cm^{-1}): from experimental data (left panel) and from computer simulations of the three models (right panel). The dashed lines in the experimental data show the results measured with He beam path while small dots show the data measured in the small angle scattering regime. The OPLS force field data is shown in full lines, CHARMM data in dotted lines and GROMOS data in dashed lines.

Very small experimental scattering pre-peaks are observed in contrast with the relatively high ones observed for mono-ols.[15] Of the simulation data, only the OPLS model displays clear pre-peaks with trends similar to that from experiments but with larger amplitude.

In order to analyze the pre-peak characteristics, we subtracted the main-peak tail and then fitted the pre-peak by a Pearson VII function to extract its amplitudes A_P , pre-peak position k_P and Full Width at Half Maximum (FWHM) applying the same procedures as done in Ref.[15] for proper comparison with the mono-ols. The results of this analysis for the experimental data and the results of the OPLS model are presented in Fig.2. The error bars were determined based on the systematic error caused by the background subtraction using both the measurements with the He beam path and the ones in air.

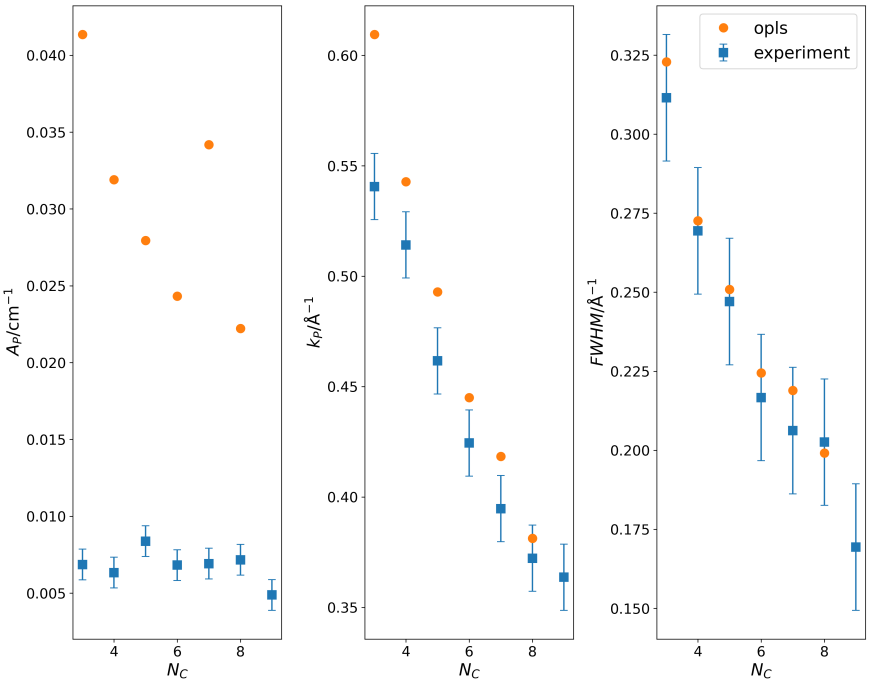

Figure 2: Comparison of pre-peak characteristics with variation of chain length N_C between experimental and OPLS results for the pre-peak. The left panel shows the pre-peak amplitudes A_P, the central panel the positions k_P and the right panel the full width at half maximum.

The experimental data show clear trends of the x-ray spectra when going from propylamine to nonylamine. The main peak intensity slightly increases with increasing length of the carbon chain N_C while its position can be found around 1.41 $\AA^{-1}$ for all amines. As evident from Fig.2, the position of the pre-peak shifts to smaller wave vector transfer k_P from 0.54 to 0.36 $\AA^{-1}$ with N_C. The amplitude of the pre-peaks lies around 0.007 cm^{-1} while their FWHM significantly decreases. These trends are similar to that observed in mono-ols, except for the pre-peak amplitude difference of nearly one order of magnitude, which we will discuss in the next sections. These trends can be explained similarly to that for alcohols.[15,16] It is the size of the methylene group that dominates the main peak, hence explaining both the position and amplitude (proportional to the number of carbons) using simple Bragg law argument. A similar argument on the size of the hydrogen bonded aggregates explains the pre-peak position, which tend to increase in size with longer amines, while the concentration of the aggregates tends to weakly diminish, considering the changes in the amplitudes and the FWHM. Particularly for the smaller amines, the pre-peak positions of the corresponding mono-ols are found to be at larger k_P which can be assigned to the larger polar groups in case of the amines.

Of the simulation data, only the OPLS model displays clear pre-peaks with trends similar to that from experimental ones, and consistent with that obtained with the same model in the case of the mono-ols. These pre-peaks are smaller than those of the mono-ols, but still a factor 5 (butylamine) to 3 (octylamine) too high when compared with the experimental data. The trend in pre-peak position with increasing chain length is reasonably well reproduced by the OPLS model. The fact that the calculated spectra are not in so much good agreement with the experimental ones as it is for monols[15] will be analyzed in the Discussion section7 .

In contrast, both CHARMM and GROMOS force fields do not show clear pre-peaks, except for the propylamine GROMOS data**.** The CHARMM model being an all-atom model, one would expect the data to be closer to that from the experiments, but this does not appear to be case in a clear fashion.

How to explain this near absence of pre-peaks in these last 2 models, as well as the contrasting results across models? In fact, it is the weakness of the pre-peak in the experiments that guides the interpretation. Because the main question is rather: why the pre-peak for amines is so small when compared to the mono-ols? Indeed, the weakness of the pre-peak might be due to weak hydrogen bond clustering of the amine head group when compared with that of the hydroxyl group. In this case, some models might exaggerate this clustering while other might totally underestimate it. The answer is neither, and lies on the nature of the charge ordering, as we will explain in Section 4.

Since in classical simulations, the hydrogen bonding is brought down to a mere Coulomb association, one could compare the partial charges on the amine group nitrogen and hydrogen atoms, as displayed in tables S2 to S6 of the SI document, to those of the hydroxyl group oxygen and hydrogen atoms, as reported in the tables S1 and S2 of Ref.[15] Such a comparison would allow to quantify the "strength" of the Hbond in amines versus alcohols. The partial charge on the nitrogen atom is in the range $q_N \approx -0.9$ to -1.0, with a 10% difference across models, while that on the oxygen atoms is about $q_O \approx -0.7$, with also a 10% difference across models. That on the hydrogen atom is about $+0.370$ for the amines and $+0.420$ for the alcohols, with again about 10% difference across models in both cases. Then, the magnitude of the cross charge product $|q_- \times q_+|$ is about 0.35 for the amines and 0.294 for the alcohols, leading to a slight advantage for the amine Hbonding over that for the hydroxyl head. In other words, the strength of the Hbond alone cannot explain the weakness of the pre-peak in the amines, since other factors come into play such as the geometry of the molecule or the packing constraints. These may either promote or prevent Hbonding, the latter which explain weaker bonds.

3.2 Clustering of the amine groups

The clustering of the amine groups can be studied from computer simulations, either by direct probing of the cluster distribution probability $P_n(s)$ for cluster size s of amine alkyl chain rank n, or by looking at snapshots from various spatial configurations, and finally by analysing the pair distribution functions

of the amine atoms and the corresponding structure factor. The calculation of the $P_n(s)$ is made by specifying the bonding distance between two nitrogen atoms, which varies up to $3.7\mathring{A}$.

Fig.3 shows the $P_n(s)$ as function of the cluster size s, for different alkylamines ($n = 3, .., 8$) and different force field models. A similar figure for the alcohol from Ref.[15] (gathered from the oxygen atoms inter-distance) is shown in Fig.S1 of the SI document. The important difference with mono-ols is that these cluster probability distributions do not have the characteristic pentamer maximum found for all mono-ols.[15,16] Instead, we find an exponential shape very similar to that of water.[67,68] This finding is related to the geometrical proximity of the Y-shaped polar heads, NH_2 for amines and OH_2 for water, the importance of which will be discussed later in the paper.

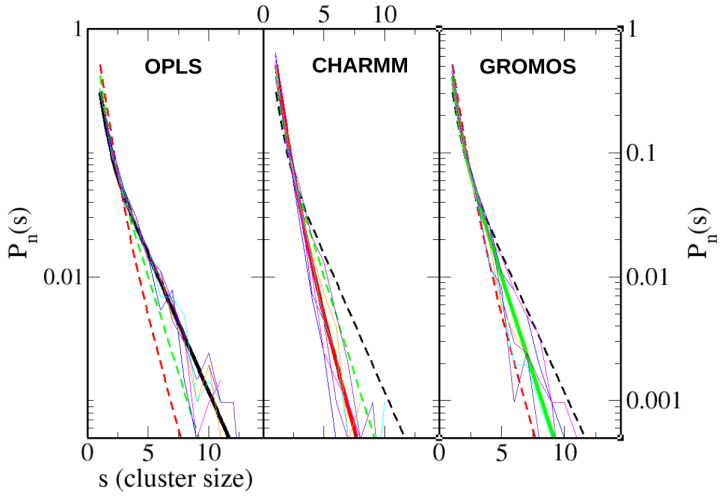

Figure 3: Cluster size s probability distribution functions $P_n(s)$ for each model in separate panels, and for different alkylamines ($n = 3, .., 8$) in each of the panels. The fits from Eq.(4) are shown as thick lines, black for OPLS, red for CHARMM and green for GROMOS. Full lines are used for the model represented in the panel, with dashed curves for the two other models.

A closer look at Fig.3 shows appreciable differences between models, with the OPLS model tending to have less monomers and more higher n-mers, the CHARMM model having the opposite trend and the GROMOS model is between the two others. All models show very weak alktl tail dependence. This is exemplified by the calculation of the average cluster size, as shown in Fig.S2 of the SI document, which show clearly the weak dependence of the alkyl tail. Therefore, we have considered that the n-dependence for amines is less important than the model dependence, and could be neglected in the following discussion. Then, the hierarchy between the 3 models is further exemplified by the 2-exponential fits of Eq.4, shown in Fig.3 in thick lines, the black line for

OPLS being above the GROMOS green curve and the CHARMM red curve.

The cluster distribution data can be fitted to a two exponential form:

$$P_n(s) = \exp(a_1 - b_1 s) + \exp(a_2 - b_2 s) \tag{4}$$

where the parameters a_k and b_k are given in Table S1 of the SI document. The n-independence of $P_n(s)$ suggests that the amine head groups cluster sizes are very similar across different amines.

3.3 Typical cluster shapes

From the computer simulations we can extract typical cluster shapes as given by our cluster extraction program. Most abundant clusters are dimers of the hydrogen bonded amine groups, such as that in Fig.3. But there are also larger clusters, as shown in Fig.(3), although their probability decrease exponentially (See Eq.(4)). The figure shows how the alkyl tails decorrelate from the amine cluster backbone.

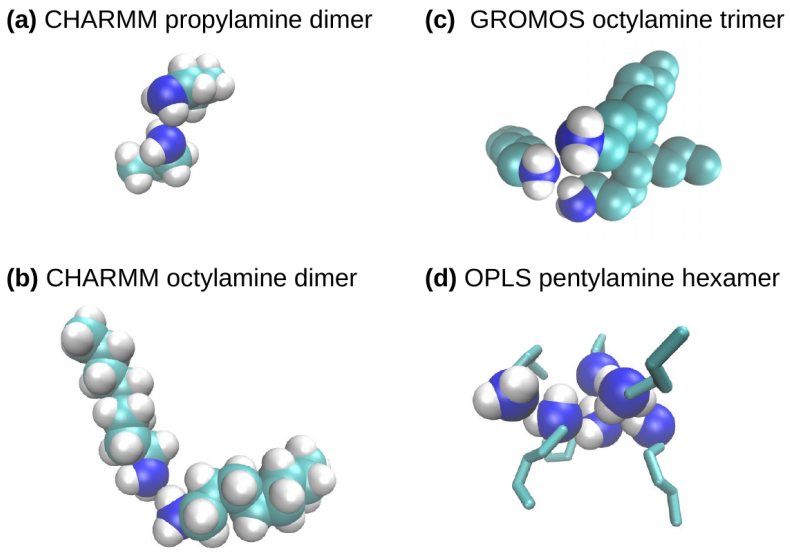

Figure 4: Typical clusters for different force field models. In (d), the alkyl tail is represented in the VMD licorice convention in order not to block the view of the amine head group chain cluster.

These figures also show how the hydrogen bonding with amines is not similar to water, because of the presence of the alkyl group which prevent tetrahedral distribution of the amine head groups. This is also probably the reason why clusters are small. It is also seen that chain clusters of the amines are not the only possibility, and that bulky groups exists, such as that in (c). OPLS has

more clear chain clustering, as seen in (d), although in practice it is mostly dimers that are found.

4 Charge order analysis through the order parameter functions

In disordered liquids, the order parameter (in the sense of the Landau free energy[69]) is the density[70] , which is just a number $\rho_a = N_a/V$ (N_a is the number of particle of species a per volume V), and will not provide any information about the microscopic structure of the liquids. Yet, associating liquids exhibit strong local order, and this shortcoming from the theoretical perspective might seem disappointing at first. However, the density ρ is in fact the one-body function $\rho_a^{(1)}(\mathbf{x})$ for species a, which has a meaning for interfacial or orientationally ordered liquids since these type of systems require a general spatial variable $\mathbf{x}$, the latter which represents the position and/or orientation of a particle, but is absent in disordered liquids since there is no preferred position or orientation. In the absence of a meaningful one-body function, one may turn to the next function in the hierarchy, which is the two-body function $\rho_{ab}^{(2)}(\mathbf{x}_1, \mathbf{x}_2)$ for a pair of species a and b, which formally defines the pair correlation function $g_{ab}(\mathbf{x}_1, \mathbf{x}_2)$ by the relation[71]

$$\rho_{ab}^{(2)}(\mathbf{x}_1, \mathbf{x}_2) = \rho_a^{(1)}(\mathbf{x}_1)\rho_b^{(1)}(\mathbf{x}_2)g_{ab}(\mathbf{x}_1, \mathbf{x}_2) \tag{5}$$

but for the type of usual disordered liquids becomes

$$\rho_{ab}^{(2)}(\mathbf{x}_1, \mathbf{x}_2) = \rho_a \rho_b g_{ab}(r) \tag{6}$$

where $r = |\mathbf{r}_1 - \mathbf{r}_2|$ is the relative distance between the 2 particles (where we consider only distances $\mathbf{r}$ without including orientations as with $\mathbf{x}$ variables). In case of disordered molecular liquids, the order parameter $g_{ab}(r)$ represents the pair distribution function between 2 atoms a and b, where it is assumed to consider the molecular liquid as a "soup" of atoms, and the intra-molecular part $w_{ab}(r)$ has been introduced in Section 2.2. This way, the molecular liquid is seen ordered through the partial charges on the atoms, constrained by the intra-molecular bonds.

The hydrogen bonding between the amine groups NH_2 are then simply a Coulomb association between two negatively charged nitrogen atoms N through one of the positively charged hydrogen atom H, similarly to the hydrogen bonding between the hydroxyl OH group in alkanols .[15] The charges for all models and all amines are displayed in the SI document in tables S2-S6. Charge order is then a classical version of the quantum physics of the hydrogen bonding between 2 molecules. However, it also allows to describe in a unified way both the molecular hydrogen bonding and the Coulomb association with ionic species. This approach is conceptually supported by the fact that the order parameter function $g_{ab}(r)$ has a characteristic shape for atoms that are associated through charge ordering, depending of the nature of the valences[72] .

4.1 Charge order and scattering

In order to demonstrate the influence of charge ordering on the x-ray scattering intensity $I(k)$, we separate in Eq.(1) the amine polar head group contributions $I_{AA}(k)$ from that of the alkyl tail $I_{TT}(k)$, as well as the cross contributions $I_{AT}(k)$, with

$$I(k) = I_{AA}(k) + I_{AT}(k) + I_{TT}(k) \tag{7}$$

These 3 contributions are shown in Fig.(5) for propylamine, together with the total intensity $I(k)$(black curves).

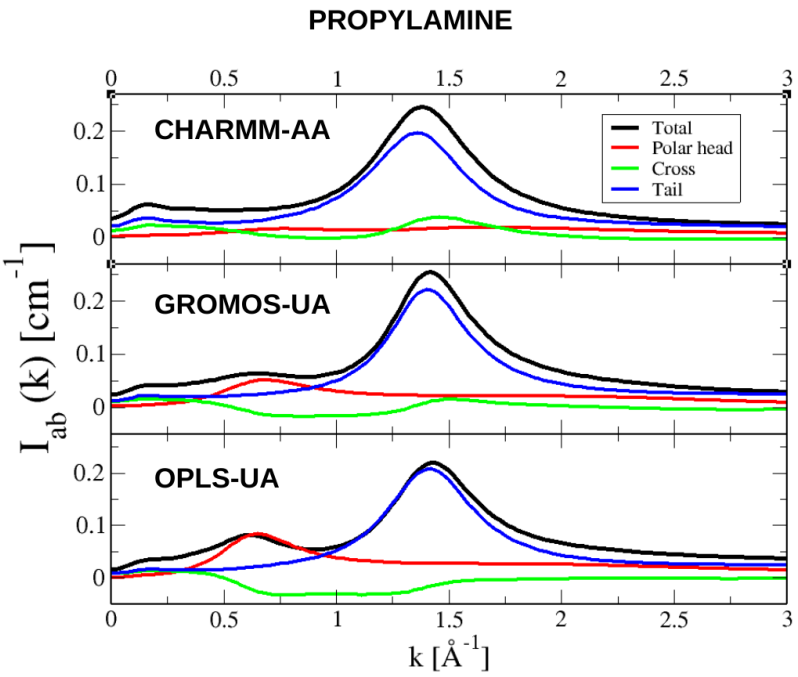

Figure 5: Partial scattering contributions for propylamine. The top panel is for the CHARMM force field, the middle panel for GROMOS and the lower panel for the OPLS model. The color codes for the curves are explicited in the inset of the topmost panel.

Since propylamine is the only amine which shows a clear weak pre-peak in x-ray scattering for both united atom force field models, it is interesting to see which part contributes mostly to it. For GROMOS and the OPLS force fields, it is the polar head contribution which dominates, while the cross contributions tend to be negative around $1\mathring{A}^{-1}$. We also note that it is the alkyl tail which contributes essentially to the main peak for all force field models, since it contains most atoms, with size $\sigma_{CH_2} \approx 4.5\mathring{A}$ corresponding to the main peak position $k = 2\pi/\sigma_{CH_2} \approx 1.4\mathring{A}^{-1}$.

A similar picture is shown for octylamine in Fig.6, and that for pentylamine is shown in the SI document Fig.S6. While the total intensity remains nearly the same as for propylamine, we notice that the partial contributions are quite different, specially in the pre-peak area. In other words, the quasi similarities between all amine scattering patterns noticed from Fig.1 hides appreciable differences between the contributions from the different molecular parts of different amines.

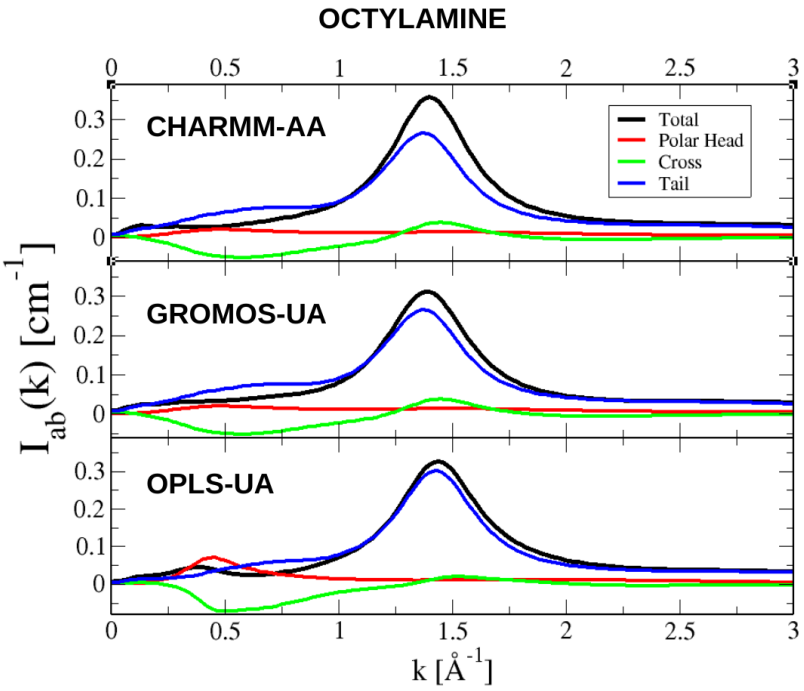

Figure 6: Partial scattering contributions for octylamine. The panels are as in Fig.5

Going into details, we see that it is the alkyl tail which contributes mostly to the main peak. These contributions differ from one model to another, and appear more important for the all-atom models. Perhaps the most interesting part is the canceling contribution from the cross and polar/non-polar contributions to the pre-peak, which are more important for the OPLS model. These cancellations are typical of charge ordering, as will be shown from the study of the pair correlation functiond and structure factors in the next sub-section. This type of cancellation occurs in ionic liquids[72] and more particularly in room temperature ionic liquids which have been the focus of recent studies from charge ordering perspective.[73–75]

It is instructive to examine these canceling contributions in alcohols, in comparison with the present ones, and particularly so for the pre-peak. This is

illustrated in Fig.S7 of the SI document in the case of the OPLS models for 1-propanol and 1-octanol, for which the differences in the pre-peak region are more marked and better shaped. However, the negative cross contribution for the alcohols appears to be somewhat less significant than for amines, which explains why the resulting pre-peak is more prominent in alcohol. However, it does not explain neither the origin of the magnitudes, nor the larger negative contributions. It is the analysis in the next section of the details of the correlation functions which can provide a complete microscopic picture for the origin of the pre-peak and its magnitude.

4.2 Study of the order parameters

Herein, the site-site correlation functions and corresponding structure factors are considered as generalized Landau-type order parameters for complex disorder liquids. The order they witness is not a global order, as in true phase transition, but the local order generated by charge ordering, which differs from that of simple disorder liquids[76,77] . In charge ordering, the alternation of the positive and negative charges leads to a typical dephasing between the $+-$ correlations and the $++ \backslash --$ correlations.[72,78] When charges are tied into molecules, charge order will condition the micro-structure at molecular level. It is an open question whether or not the resulting site-site correlations will still obey this dephasing, and to what extent. In mono-ols, it was shown that charge order and dephasing of charge-charge correlations are still respected. Since, from the studies above, it appears that the amine groups tend to show less charge order than mono-ols and favour mostly dimers, it is interesting to examine in Fig.(7) the charge order of the amine head group nitrogen N and hydrogen atoms H, charged negatively and positively, respectively.

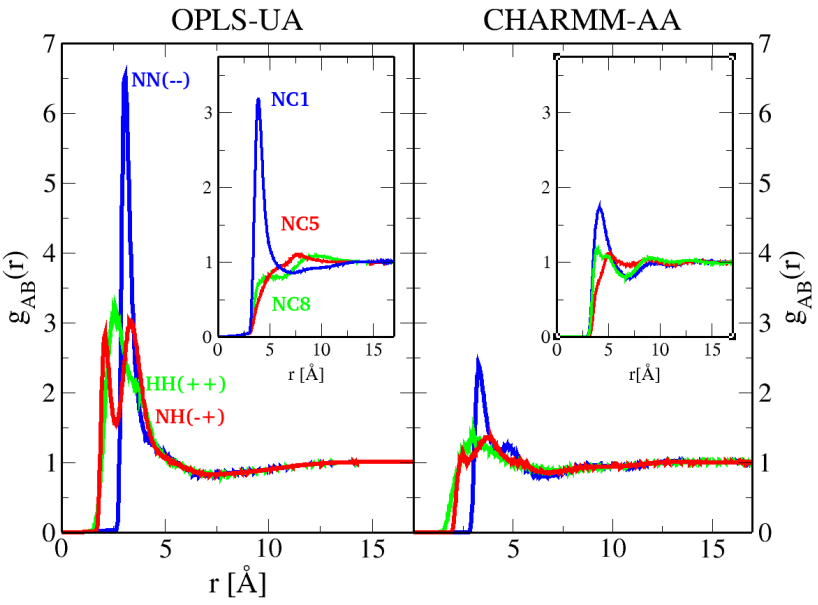

Figure 7: Charge order of the amine NH_2 head group atoms for octylamine, from the point of view of the site-site correlation functions. The inset shows the nitrogen-carbon NC_n cross correlations between the first C_1 , the fifth C_5 and last carbon C_8 groups. See text for more details.

Since the OPLS model (left panel) shows a marked pre-peak similar to that in mono-ols, we observe a clear charge ordering, with the typical phase opposition between the N(-)H(+) correlation and the H(+)H(+) or N(-)N(-) correlations. Incidentally, because of the double hydrogens, $g_{NH}(r)$ has a double peak since the amine head can equally bond with the 2 hydrogen atoms. This is because the alkyl tail blocks the tetrahedral order which would allow to separate the bonding with the 2 hydrogens. This is a topological constraint. The CHARMM model (right panel) has very clearly less marked charge order correlation, seen through the lesser amplitude of the peaks, although these are there and obey similar dephasing. The $g_{NN}(r)$ has a main peak with a smaller shoulder peak around $r \approx 5\mathring{A}$, which is probably a second hydrogen bonding with another nitrogen. This is also a consequence of the topological constraints, modified by the less localized bonding possibility, precisely because of the weaker bonding than in OPLS.

Fig.S3 of the SI document shows the corresponding figure for OPLS octanol (left panel). While very similar features can be observed, one notes the much higher amplitudes in the charged atom correlations, indicating that charge order is more pronounced for alcohols. In particular, the difference in height of first double peak in the NH correlations (red curve) for amines, compared with the asymmetry for the alcohol, corresponds to the different topologies of the amine

and hydroxyl groups.

Fig.8 shows the atom-atom structure factors corresponding to the correlations shown in Fig.7, for both models. Again, the similarity with the same correlations in 1-octanol are really striking (see Fig.S3 and Fig.S5 in the SI document). This similarity is not limited to 1-octanol and lower amines can equally be compared with lower alcohols. We note that all amine group atoms pairs have the same pre-peak, which is more marked for OPLS than for CHARMM, as expected. This is a consequence of the fact that all atoms in the amine group pilot the charge ordering in the same way. Despite small differences observed in the r-space correlations between near neighbours, the collective effect at large r is very similar, which translate in a unique pre-peak in k-space. This feature illustrates the necessity to look at both the r-space and reciprocal space correlation order parameters.

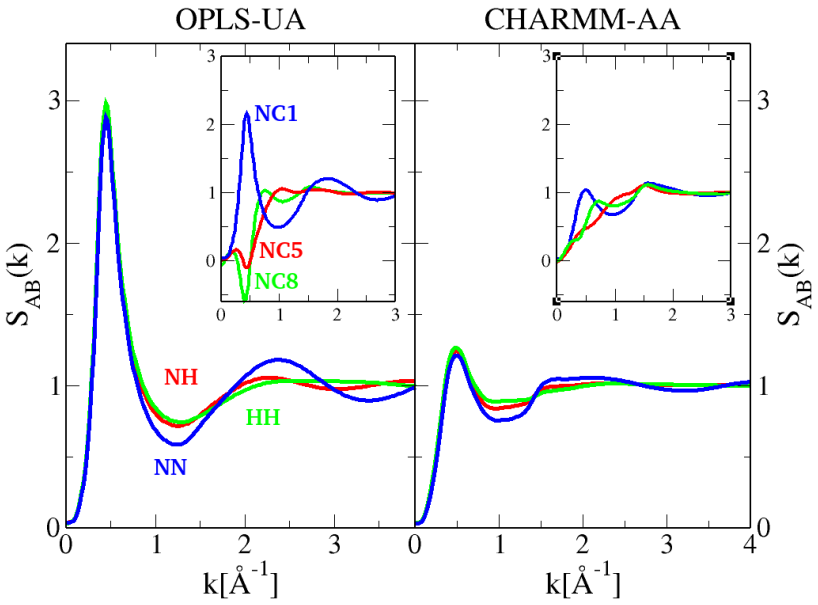

Figure 8: Charge order of the amine head group atoms for octylamine, from the point of view of the site-site structure factors. The inset shows the structure factors between the nitrogen atom and first C_1 , fifth C_5 and last C_8 carbon groups. See text for more details.

It is also important to remind the physical and mathematical origin of the pronounced pre-peak, which we have introduced in Ref.,[76] and observed in subsequent works.[15,16] In these systems we are concerned with, scattering pre-peaks are generated by chain clustering of the hydrogen bonding groups (OH in alcohols and NH in amines). This particular form of clustering can be seen from 2 features in the pair correlation functions. The first feature is a narrow and

prominent first peak, which has two meaning: the height indicates the strength of the H-bonding, while the width indicates the "looseness" of the H-bonding directionality. The second feature is the relatively shallow depletion following this first peak, and which extends far beyond it. These 2 features can be clearly seen in the left panel of Fig.7 for the OPLS $g_{NN}(r)$, and they are much less marked for the CHARMM model. From this, we are able to conclude that the OPLS model has more and longer N-H chain clustering than the CHARMM model, which might explain the more prominent scattering pre-peak.

Turning now to the insets of both figures 7 and 8, these represent the cross correlations between the nitrogen atom and selected tail carbon atoms, namely the first C_1, fifth C_5 and last C_8. The OPLS model illustrates in the inset of Fig.(7) how the last atom C_8 is depleted from the nitrogen with first neighbour peak below 1. This depletion leads to negative pre-peak structure factor contributions as seen on the corresponding inset of Fig.(8). This is not the case for the first carbon, since the proximity of nitrogen atoms automatically ensured that the attached first carbons as well. A similar behaviour is equally observed for alcohols, as illustrated in Fig.S3 for octanol. The amplitudes in the pre-peaks and anti-peaks are surprizingly similar. In the case of the CHARMM model, the depletion effect is much less pronounced, if not suppressed at all, indicating that charge ordering is more "disordered" for this model.

These features are shared by all amines, with variations in amplitude of the effects. For instance, in Fig.9 and Fig.10, we illustrate this similarity in the case of correlations in pentylamine.

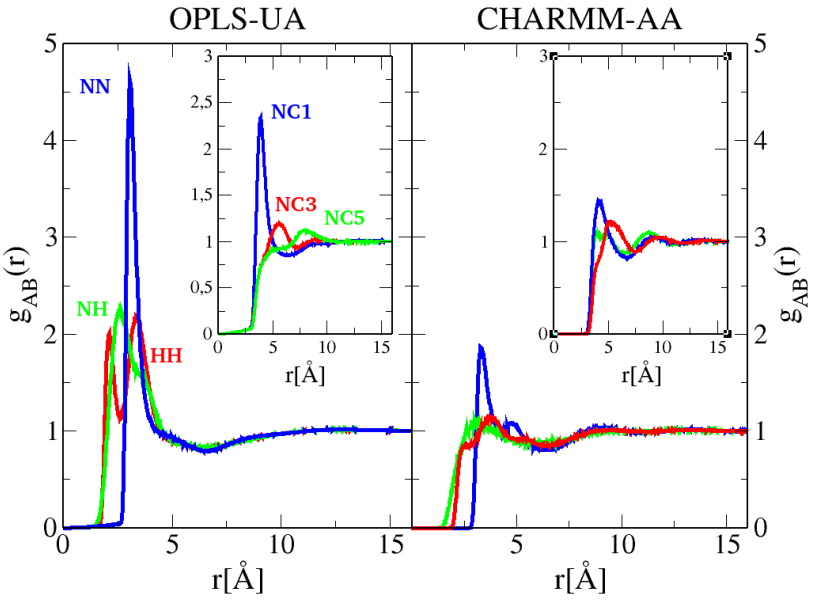

Figure 9: Charge order of the amine head group atoms for pentylamine, from the point of view of the site-site correlation functions. The inset shows the nitrogen-carbon NC_n cross correlations combinations between the first C_1 , third C_3 and last carbon C_5 groups. The color conventions are as in Fig.(7). See text for more details.

These correlation functions are very similar to the previous ones, except for an overall lesser amplitude of the charge ordering. This similarity indicates two features, that we previously noticed in mono-ols. Firstly, the amine group correlations are strikingly similar, with only small amplitude difference, despite the underlying differences between models. Secondly, the connections between the hydrogen bonding head groups and the quasi neutral tails is very important, despite the fact that the tails are expected to be more or less decorrelated around the polar head cluster.

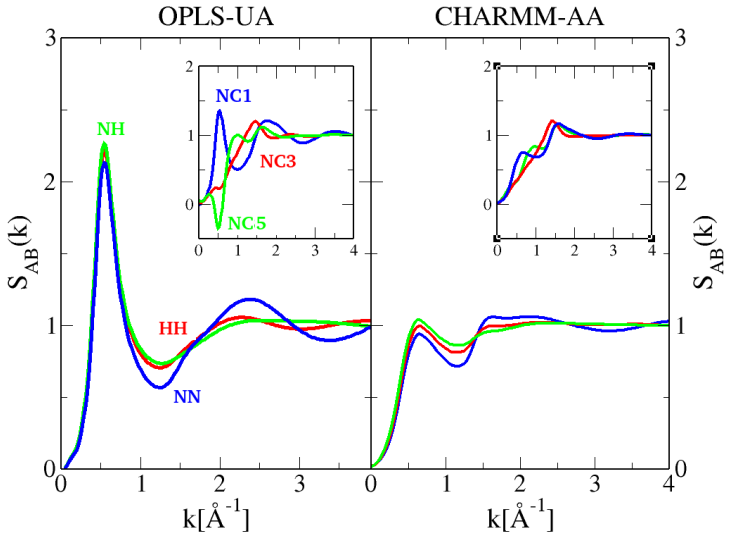

Figure 10: Charge order of the amine head group atoms for pentylamine, from the point of view of the site-site structure factors. The inset shows the structure factors between the nitrogen atom and the first C_1 , third C_3 and last C_5 carbon groups. See text for more details.

In connection with the partial scattering contributions of Fig.6, since the charge order between the alkanols and the alkylamines look quite similar, one may ask why there is no pre-peak in the amines? It appears that the amine group correlations are not so strong, while the cross polar/alkyl correlations, including their anti-correlations, are as strong as in alkanols, hence over canceling the positive correlations that would give pre-peak. This conclusion is entirely supported by the OPLS model, precisely because it has amine group correlations very similar to that of the hydroxyl group of the alkanols.

5 Force field dependence of the micro-structure of alkylamines

One important difference between the 3 force field models is the all-atom modeling of the alkyl tail of the CHARMM model, with partial charges, albeit quite small, on the carbon and hydrogen atoms. However, the GROMOS model has also partial charges in the alkyl tail. This is the main difference with the OPLS model, which has zero charges on the CH_n groups. As seen in the previous section, the absence of charges on the alkyl tail does not necessary imply that the nitrogen-alkyl tail atom cross correlations are weak (see the insets of Figs.7 to Fig.10). As stated previously, it is in fact the balance of correlations and anti-correlations between the head and tail groups which determines the exis-

tence and the strength of the pre-peak. Apparently, the higher valences of the OPLS model somehow compensate the absence of charges on the tail atoms.

We compare below the correlations of the nitrogen atom, which is central to the hydrogen bonding, between the 3 models. We focus on the amines with the smallest tail, which is propylamine, and the longest one, octylamine. Fig.11 shows the $g_{NN}(r)$ for all 3 models, for propylamine and octylamine as well as the corresponding structure factors in the insets.

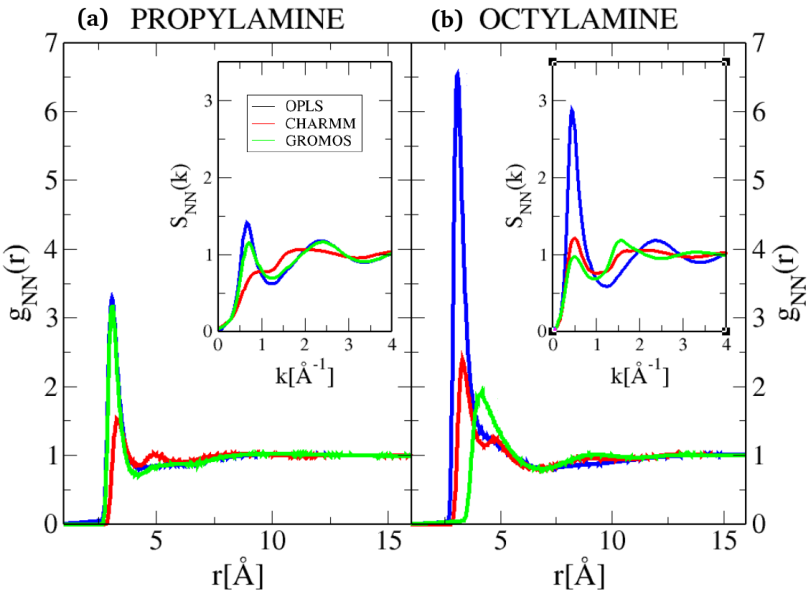

Figure 11: Nitrogen-nitrogen correlation function for propylamine (a) and octylamine (b). The corresponding structure factors are shown in the insets.

We note that there are important differences between the short range correlations of the alkylamines, which are common to all 3 models: there is a widening of the base of the first peak for the longer alkylamine, indicating that N-N contacts are both more enhanced for direct dimer pair formation (higher first peaks) and allowing higher n-mer formation, such as most probably trimers. This interpretation is supported by the larger correlation depletion range at higher distances, indicating that the separation with next N neighbours increases with alkyl tails. This is very counter-intuitive, since one would expect larger N clusters when the alkyl tails are entropically favorable, that is when they are small. Instead, it would appear that longer tails favour micelle-type at the core. In other words, longer alkylamines would tend to behave like micellar melts.

We note that this micellisation-like behaviour is less supported by the GROMOS model, since the main peak of $g_{NN}(r)$ is smaller, but also the pre-peak of $S_{NN}(k)$ is smaller than the other models.

6 Charge ordering differences between water, amines and alcohols

It is instructive to examine the charge ordering mechanism by comparing three different types of hydrogen bonding liquids, water, amines and alcohols. We note that the water molecule OH2 has a C2v symmetry in the Schönflies notation,[79] which is also that of the NH2 amine head group. This symmetry favours branching patterns. In contrast, the OH hydroxyl head group has linear symmetry, which favours chaining patterns. Both symmetries are lost when attached to the alkyl tails. However, the bonding patterns inherit these respective symmetries. This is the reason why the cluster probabilities in Fig.3 look very much like that for water, and do not have the typical peak at cluster size $s = 5$ observed for all alcohols.[15,16] The amines do not maintain the branching characteristics of C2v because of the tail. However, the C2v symmetry definitely hinders chaining patterns and makes small clusters (dimers and trimers) likely.

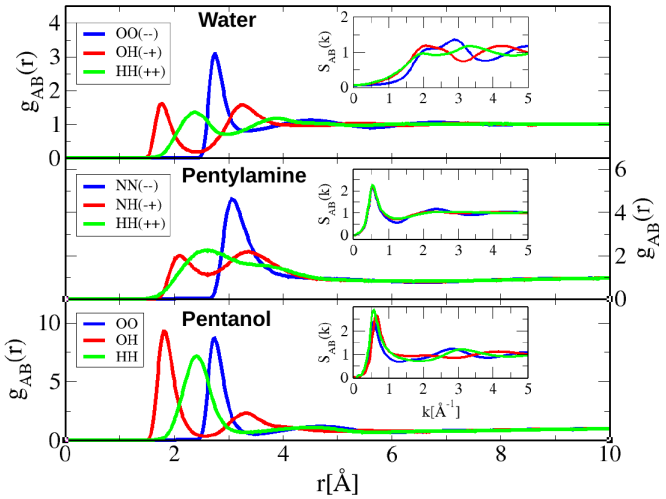

Figure 12: Compare the charge order parameters between SPC/E water (top panel), OPLS pentylamine (middle panel) and pentanol (lower panel). The respective structure factors are shown in the insets. Note that the vertical scales differ for each panels and insets.

Fig.12 compares the charge order parameters between water (SPC/E model) and pentylamine (OPLS model), base on the identity of the Schönflies C2v symmetry of the OH2 and NH2 groups. The comparison illustrates several appealing symmetries. For comparison, the same order parameters for pentanol (OPLS) are equally shown in the lower part.

The similarities between the pair correlation order parameters between water and the amine are really striking in the short range parts in the r-range

$[0-5\mathring{A}]$ where the first peaks are most apparent. The NN and NH shapes are quite similar to the OO and OH shapes. It is only the HH part which differs significantly, indicating that the alkyl tail perturbs the positioning of the hydrogen atoms, as opposed to the case of water where they are not hindered. This is very different from the pentanol, where the OH bonding has a clear strength in magnitude, favoured by the direct OHO chain bonding mechanism observed in all alcohols,[15] including those with branching tails.[16] These findings supports and confirms the symmetry argument provided above.

The depletion range part, in the r-range $[5\mathring{A}-10\mathring{A}]$ contains the depletion correlations, which do not exist for water, and which are not much visible in Fig.12 for the amine and the alcohol, because of the squashed vertical scale, but are visible for instance in Fig.11 above, and also in our paper in alcohols microstructure,[80] and in Fig.S3 and Fig.S4 of the SI document. This depletion range is more marked for the alcohol than for the amine. This is compatible with the prominent scattering pre-peak in alcohols, as opposed to weak ones in amines.

However, the structure factor order parameters totally fail this similarity argument, which seems to hold only in real space – where actual bonding occurs and spatial topologies are established. In the reciprocal space, it is more the global structure that is apparent, and clearly water and amines are not the same type of liquid. This explains the strong differences in reciprocal space. This is apparent from the near in phase correlations for the amine, and the out-of-phase correlations for water. In that, the alcohol appears as closer to the amine, and water really stands apart.

7 Discussion

This study demonstrates that presence or absence of scattering pre-peak cannot be inferred so-easily to the presence or absence of clusters in the system. Similarly, a direct cluster study may or may not reveal specific clusters as a peak in the cluster probability distribution function. It is really the order parameters, which are the correlation functions, which reveal or not if there is clustering, depending on the cancellation or not of some of pre-peaks and corresponding anti-peaks in the atom-atom structure factors. These functions are unfortunately not available from experiments (except perhaps in some very specific small angle studied of neutron scattering[81,82]). In other words, it is necessary to perform computer simulations, which means introducing approximate force fields, and some arbitrariness.

The presence (alcohols) or absence (amines) of cluster peak, brought in parallel with the correlated presence/absence of scattering pre-peaks, and in contrast with the omni-presence of cluster pre-peaks and anti-peaks in structure factors (and associated features in the correlation functions), may entice one to consider the cluster calculation as a better observable than the correlation functions. We tend to oppose this view for two reasons. Firstly, the clusters studied in both amine and alcohol systems are the result of charge ordering, a criteria which is

absent from cluster calculation. Secondly, the criteria for cluster calculations have a "covalent' character to them, whereas cluster are essentially labile in nature, and this property is most directly captured by correlation function which are related to concentration fluctuation by their very definition.[71] This issue, however, requires theoretical considerations[76–78] which are not within the scope of the present work.

We come back to the remark in Section 3.1 about the possible reasons for the better agreement of the scattering intensities with simulation data for alcohols[15] instead of amines. We would like to point out that, in fact, the differences between the experimental and simulations $I(k)$ are always there, and can be more or less prominent, depending on models. But, the fact that alcohols show a better trend for pre-peak help mask these differences. This is in relation with the cancellation feature due to the underlying charge ordering, that is always at the origin of the pre-peak. We conjecture that systems which show less or no pre-peak, are more prone to concentration fluctuations, a feature which tends to smooth out aggregates, as opposed to those which has marked pre-peaks, which have more robust and long lived aggregate structures. This can be seen as a classical equivalent of the boson-fermion symmetry, something that we have already observed in a previous recent work.[83]

This type of cancellation between different atom-atom structure factors, and driven by the charge order mechanism, may play an important role in the x-ray study of large molecules in soft-matter systems and those of biological interest, where even larger molecules such as enzymes for instance, are mixed with solvent and other smaller molecules.[84] In such cases, the disparity of sizes induce concentration fluctuations, which tend to raise the small-k part of the scattering patterns. Then, in the absence of the pre-peak, it is difficult to decide if the large scattering amplitudes at small k are a signature of concentration fluctuations alone, or hide significant clustering hidden to the experimental observation. This is for instance the case in aqueous t-butanol mixtures,[85],[86] or aqueous mixtures of small surfactant molecules.[87–89] Our present results incite to more precautions in interpreting these data, and may require revisiting many of the previous scattering results in soft-matter systems.

8 Conclusion

In this work, we have proposed to consider charge order as an important form of local order, associated to the atom-atom pair correlation functions and corresponding structure factors. We have illustrated the usefulness of this approach to understand the apparent weakness of clustering in liquid amines, as suggested by the very weak x-ray scattering pre-peaks. This concept allows to explain the magnitude of the scattering pre-peak as a competition effect between the positive correlations between the charged groups, and that of the negative correlations between the uncharged (or weakly charged ones), for given molecular topologies. In the case of the alcohols, since the OH chaining is not hindered, this competition is in favour of charged group correlations, which leads to a positive

scattering pre-peak. In the case of amines, the C2v symmetry of the head group hinders clustering, leading to a draw between the two cancelling contributions, resulting in a very small pre-peak.

The computer simulation studies of several force fields have revealed that significant H-bonding and clustering occurs in liquid amines, but that charge ordering associated to the particular symmetries of the associating atomic groups, tend to produce canceling contributions which diminish the height of the scattering intensities of the pre-peak. However, significant differences between different force fields are also found, which tend to affect the interpretation. In the case of liquid amines, no particular force field appears to be reliable, although the overall agreement is not so bad. Moreover, all force field converge as far as interpretations of the microscopic process are concerned, which is the positive side of the simulation approach.

Supporting Information

The Supporting Information document contains data comparison with mono-ols, details of cluster calculations and tables of the force field charge parameters.

Acknowledgments

We thank DELTA for providing synchrotron radiation at beamline BL2 and technical support. The help of Jaqueline Savelkous, Eric Schneider, and Dirk Lätzenkirchen-Hect is thankfully aknowledged for preparatory measurements at BL8. This work was supported by the BMBF via DAAD (PROCOPE 2024-2025, Project-ID 57704875) within the French-German collaborations PROCOPE (50951YA), *Analysis of the molecular coherence in the self-assembly process: experiment and theory.*

References

[1] Magini, M.; Paschina, G.; Piccaluga, G. On the structure of methyl alcohol at room temperature. *The Journal of Chemical Physics* **1982**. *77*, 2051–2056.

[2] Narten, A.; Habenschuss, A. Hydrogen bonding in liquid methanol and ethanol determined by x-ray diffraction. *The Journal of Chemical Physics* **1984**. *80*, 3387–3391.

[3] Sarkar, S.; Joarder, R. N. Molecular clusters and correlations in liquid methanol at room temperature. *The Journal of Chemical Physics* **1993**. *99*, 2032–2039.

[4] Sarkar, S.; Joarder, R. N. Molecular clusters in liquid ethanol at room temperature. *The Journal of Chemical Physics* **1994**. *100*, 5118–5122.

[5] Vahvaselkä, K. S.; Serimaa, R.; Torkkeli, M. Determination of liquid structures of the primary alcohols methanol, ethanol, 1-propanol, 1-butanol and 1-octanol by x-ray scattering. *Journal of Applied Crystallography* **1995**. *28*, 189–195.

[6] Karmakar, A.; Krishna, P.; Joarder, R. On the structure function of liquid alcohols at small wave numbers and signature of hydrogen-bonded clusters in the liquid state. *Physics Letters A* **1999**. *253*, 207–210.

[7] Akiyama, I.; Ogawa, M.; Takase, K.; Takamuku, T.; Yamaguchi, T.; Ohtori, N. Liquid structure of 1-propanol by molecular dynamics simulations and x-ray scattering. *Journal of Solution Chemistry* **2004**. *33*, 797–809.

[8] Tomšič, M.; Jamnik, A.; Fritz-Popovski, G.; Glatter, O.; Vlček, L. Structural properties of pure simple alcohols from ethanol, propanol, butanol, pentanol, to hexanol: Comparing monte carlo simulations with experimental saxs data. *The Journal of Physical Chemistry B* **2007**. *111*, 1738–1751.

[9] Cerar, J.; Lajovic, A.; Jamnik, A.; Tomšič, M. Performance of various models in structural characterization of n-butanol: Molecular dynamics and x-ray scattering studies. *Journal of Molecular Liquids* **2017**. *229*, 346 – 357.

[10] Bakó, I.; Jedlovszky, P.; Pálinkás, G. Molecular clusters in liquid methanol: a reverse monte carlo study. *Journal of Molecular Liquids* **2000**. *87*, 243–254.

[11] Kosztolányi, T.; Bakó, I.; Pálinkás, G. Hydrogen bonding in liquid methanol, methylamine, and methanethiol studied by molecular-dynamics simulations. *The Journal of Chemical Physics* **2003**. *118*, 4546–4555.

[12] Ludwig, R. The structure of liquid methanol. *ChemPhysChem* **2005**. *6*, 1369–1375.

[13] Benmore, C.; Loh, Y. The structure of liquid ethanol: A neutron diffraction and molecular dynamics study. *The Journal of Chemical Physics* **2000**. *112*, 5877–5883.

[14] Lehtola, J.; Hakala, M.; Hämäläinen, K. Structure of liquid linear alcohols. *The Journal of Physical Chemistry B* **2010**. *114*, 6426–6436.

[15] Požar, M.; Bolle, J.; Sternemann, C.; Perera, A. On the x-ray scattering pre-peak of linear mono-ols and the related microstructure from computer simulations. *J. Phys. Chem. B* **2020**. *124*, 8358–8371.

[16] Bolle, J.; Bierwirth, S. P.; Požar, M.; Perera, A.; Paulus, M.; MÃŒnzner, P.; Albers, C.; Dogan, S.; Elbers, M.; Sakrowski, R.; et al. Isomeric effects in structure formation and dielectric dynamics of different octanols. *Phys. Chem. Chem. Phys.* **2021**. *23*, 24211–24221.

[17] Frank, H. S. The structure of ordinary water. *Science* **1970**. *169*, 635–641.

[18] Stillinger, F. H. Water revisited. *Science* **1980**. *209*, 451–457.

[19] Ohmine, I.; Tanaka, H. Fluctuation, relaxations, and hydration in liquid water. hydrogen-bond rearrangement dynamics. *Chem. Rev.* **1993**. *93*, 2545–2566.

[20] Mishima, O.; Stanley, H. E. The relationship between liquid, supercooled and glassy water. *Nature* **1998**. *396*, 329–335.

[21] Head-Gordon, T.; Hura, G. Water structure from scattering experiments and simulation. *Chem. Rev.* **2002**. *102*, 2651–2670.

[22] Stanley, H. E.; Kumar, P.; Franzese, G.; Xu, L.; Yan, Z.; Mazza, M. G.; Buldyrev, S. V.; Chen, S.-H.; Mallamace, F. Liquid polyamorphism: Possible relation to the anomalous behaviour of water. *The European Physical Journal Special Topics* **2008**. *161*, 1–17.

[23] Gallo, P.; Amann-Winkel, K.; Angell, C. A.; Anisimov, M. A.; Caupin, F.; Chakravarty, C.; Lascaris, E.; Loerting, T.; Panagiotopoulos, A. Z.; Russo, J.; et al. Water: A tale of two liquids. *Chemical Reviews* **2016**. *116*, 7463–7500. PMID: 27380438.

[24] Perera, A. On the microscopic structure of liquid water. *Molecular Physics* **2011**. *109*, 2433–2441.

[25] Gorzynski Smith, J. *General, organic, and biological chemistry*. McGraw-Hill, New York, 1st ed., **2010**.

[26] Freed, S.; Jacobson, H. F. On the Symmetries of the Fields About Ions in Solution. Equilibrium between Forms of Different Symmetry. *The Journal of Chemical Physics* **1938**. *6*, 654–655.

[27] Almásy, L.; Kuklin, A.; Požar, M.; Baptista, A.; Perera, A. Microscopic origin of the scattering pre-peak in aqueous propylamine mixtures: X-ray and neutron experiments versus simulations. *Phys. Chem. Chem. Phys.* **2019**. *21*, 9317–9325.

[28] Maloney, A. G. P.; Wood, P. A.; Parsons, S. Competition between hydrogen bonding and dispersion interactions in the crystal structures of the primary amines. *CrystEngComm* **2014**. *16*, 3867–3882.

[29] Sacharczuk, N.; Olejniczak, A.; Bujak, M.; Podsiadlo, M. Polymorphism, intermolecular interactions, and properties of primary amines at high pressure. *Crystal Growth and Design* **2023**. *23*, 7119–7125.

[30] Kusalik, P. G.; Bergman, D.; Laaksonen, A. The local structure in liquid methylamine and methylamine–water mixtures. *The Journal of Chemical Physics* **2000**. *113*, 8036–8046.

[31] Kosztolányi, T.; Bakó', I.; Pálinkás, G. Hydrogen bonding in liquid methanol, methylamine, and methanethiol studied by molecular-dynamics simulations. *The Journal of Chemical Physics* **2003**. *118*, 4546–4555.

[32] Bauer, B. A.; Patel, S. Condensed-phase properties of n-alkyl-amines from molecular dynamics simulations using charge equilibration force fields. *Journal of Molecular Liquids* **2008**. *142*, 32–40.

[33] Orozco, G. A.; Nieto-Draghi, C.; Mackie, A. D.; Lachet, V. Transferable force field for equilibrium and transport properties in linear, branched, and bifunctional amines i. primary amines. *The Journal of Physical Chemistry B* **2011**. *115*, 14617–14625. PMID: 22034922.

[34] Orozco, G. A.; Nieto-Draghi, C.; Mackie, A. D.; Lachet, V. Transferable force field for equilibrium and transport properties in linear and branched monofunctional and multifunctional amines. ii. secondary and tertiary amines. *The Journal of Physical Chemistry B* **2012**. *116*, 6193–6202. PMID: 22551443.

[35] Orozco, G. A.; Nieto-Draghi, C.; Mackie, A. D.; Lachet, V. Equilibrium and transport properties of primary, secondary and tertiary amines by molecular simulation. *Oil and Gas Science and Technology, Revue d'IFP Energies nouvelles* **2014**. *69*, 833–849.

[36] Orozco, G. A.; Lachet, V.; Mackie, A. D. Physical absorption of green house gases in amines: The influence of functionality, structure, and cross-interactions. *The Journal of Physical Chemistry B* **2016**. *120*, 13136–13143. PMID: 27966955.

[37] Guevara-Carrion, G.; Vrabec, J.; Hasse, H. On the prediction of transport properties of monomethylamine, dimethylamine, dimethylether and hydrogen chloride by molecular simulation. *Fluid Phase Equilibria* **2012**. *316*, 46–54.

[38] Castro-Anaya, L. E.; Orozco, G. A. Self-diffusion coefficients of amines, a molecular dynamics study. *Fluid Phase Equilibria* **2022**. *553*, 113301.

[39] Narimani, M.; Amjad-Iranagh, S.; Modarress, H. Performance of tertiary amines as the absorbents for co2 capture: Quantum mechanics and molecular dynamics studies. *Journal of Natural Gas Science and Engineering* **2017**. *47*, 154–166.

[40] Sharif, M.; Zhang, T.; Wu, X.; Yu, Y.; Zhang, Z. Evaluation of co2 absorption performance by molecular dynamic simulation for mixed secondary and tertiary amines. *International Journal of Greenhouse Gas Control* **2020**. *97*, 103059.

[41] Sinehbaghizadeh, S.; Saptoro, A.; Naeiji, P.; Mohammadi, A. H. Molecular dynamics simulations to investigate the effects of organic amines on biogas clathrate hydrate formation. *Journal of Molecular Liquids* **2023**. *382*, 122015.

[42] Adisa, B.; Bruce, D. A. Molecular dynamics simulations of helix-forming, amine-functionalized m-poly (phenyleneethynylene) s. *The Journal of Physical Chemistry B* **2005**. *109*, 7548–7556.

[43] Estridge, C. E. The effects of competitive primary and secondary amine reactivity on the structural evolution and properties of an epoxy thermoset resin during cure: A molecular dynamics study. *Polymer* **2018**. *141*, 12–20.

[44] Afsharhashemkhani, S.; Jamal-Omidi, M. Investigating the effect of chemical structures on water sorption and diffusion in amine-cured epoxy resins by molecular dynamics simulations. *Computational Materials Science* **2024**. *235*, 112809.

[45] Krywka, C.; Sternemann, C.; Paulus, M.; Javid, N.; Winter, R.; Al-Sawalmih, A.; Yi, S.; Raabe, D.; Tolan, M. The small-angle and wide-angle X-ray scattering set-up at beamline BL9 of DELTA. *Journal of Synchrotron Radiation* **2007**. *14*, 244–251.

[46] Hammersley, A.; Svensson, S.; Hanfland, M.; Fitch, A.; D.Hausermann. Two - dimensional detector software: From real detector to idealised image or two-theta scan. *High Pressure Research* **1996**. *14*, 235–248.

[47] Dargasz, M.; Bolle, J.; Faulstich, A.; Schneider, E.; Kowalski, M.; Sternemann, C.; Savelkouls, J.; Murphy, B.; Paulus, M. X-ray scattering at beamline bl2 of delta: Studies of lysozyme-lysozyme interaction in heavy water and structure formation in 1-hexanol. *Journal of Physics: Conference Series* **2022**. *2380*, 012031.

[48] Pronk, S.; Páll, S.; Schulz, R.; Larsson, P.; Bjelkmar, P.; Apostolov, R.; Shirts, M.; Smith, J.; Kasson, P.; van der Spoel, D.; et al. Gromacs 4.5: a high-throughput and highly parallel open source molecular simulation toolkit. *Bioinformatics* **2013**. *29*, 845–854.

[49] Požar, M.; Perera, A. On the micro-heterogeneous structure of neat and aqueous propylamine mixtures: A computer simulation study. *Journal of Molecular Liquids* **2017**. *227*, 210.

[50] Oostenbrink, C.; Soares, T. A.; Van Der Vegt, N. F.; Van Gunsteren, W. F. Validation of the 53a6 gromos force field. *European Biophysics Journal* **2005**. *34*, 273–284.

[51] Malde, A. K.; Zuo, L.; Breeze, M.; Stroet, M.; Poger, D.; Nair, P. C.; Oostenbrink, C.; Mark, A. E. An automated force field topology builder (atb) and repository: Version 1.0. *Journal of Chemical Theory and Computation* **2011**. *7*, 4026–4037.

[52] Vanommeslaeghe, K.; Hatcher, E.; Acharya, C.; Kundu, S.; Zhong, S.; Shim, J.; Darian, E.; Guvench, O.; Lopes, P.; Vorobyov, I.; et al. Charmm general force field: A force field for drug-like molecules compatible with the charmm

all-atom additive biological force fields. *Journal of Computational Chemistry* **2010**. *31*, 671–690.

[53] Vanommeslaeghe, K.; MacKerell, A. D. Automation of the charmm general force field (cgenff) i: Bond perception and atom typing. *Journal of Chemical Information and Modeling* **2012**. *52*, 3144–3154.

[54] Vanommeslaeghe, K.; Raman, E. P.; MacKerell, A. D. Automation of the charmm general force field (cgenff) ii: Assignment of bonded parameters and partial atomic charges. *Journal of Chemical Information and Modeling* **2012**. *52*, 3155–3168.

[55] Schmid, N.; Eichenberger, A.; Choutko, A.; Riniker, S.; Winger, M.; Mark, A.; van Gunsteren, W. Definition and testing of the gromos force-field versions 54a7 and 54b7. *European Biophysics Journal* **2011**. *40*, 843.

[56] Jorgensen, W.; Maxwell, D.; Tirado-Rives, J. Development and testing of the opls all-atom force field on conformational energetics and properties of organic liquids. *Journal of the American Chemical Society* **1996**. *118*, 11225.

[57] Jorgensen, W. Optimized intermolecular potential functions for liquid alcohols. *The Journal of Physical Chemistry* **1986**. *90*, 1276.

[58] Martínez, J.; Martínez, L. Packing optimization for automated generation of complex system's initial configurations for molecular dynamics and docking. *Journal of Computational Chemistry* **2003**. *24*, 819.

[59] Bussi, G.; Donadio, D.; Parrinello, M. Canonical sampling through velocity rescaling. *The Journal of Chemical Physics* **2007**. *126*, 014101.

[60] Parrinello, M.; Rahman, A. Crystal structure and pair potentials: A molecular-dynamics study. *Physical Review Letters* **1980**. *45*, 1196.

[61] Parrinello, M.; Rahman, A. Polymorphic transitions in single crystals: A new molecular dynamics method. *Journal of Applied Physics* **1981**. *52*, 7182.

[62] Hockney, R. *Methods in computational physics, vol. 9*, Orlando Academic Press, vol. 9, chap. The potential calculation and some applications, 135–221. **1970**.

[63] Darden, T.; York, D.; Pedersen, L. Particle mesh ewald: An n*log(n) method for ewald sums in large systems. *The Journal of Chemical Physics* **1993**. *98*, 10089.

[64] Hess, B.; Bekker, H.; Berendsen, H.; Fraaije, J. Lincs: A linear constraint solver for molecular simulations. *Journal of Computational Chemistry* **1997**. *18*, 1463.

[65] Debye, P. Zerstreuung von röntgenstrahlen. *Annalen der Physik* **1915**. *351*, 809–823.

[66] Debye, P. Scattering of x-rays. In *The collected papers of Peter J.W. Debye*, Interscience Publishers. **1954**.

[67] Zoranić, L.; Sokolić, F.; Perera, A. Microstructure of neat alcohols: A molecular dynamics study. *The Journal of Chemical Physics* **2007**. *127*, 024502.

[68] Perera, A.; Sokolić, F.; Zoranić, L. Microstructure of neat alcohols. *Physical Review E* **2007**. *75*, 060502(R).

[69] Landau, L. D.; Lifshitz, E. M. *Statistical Physics, Part 1*, vol. 5 of *Course of Theoretical Physics*. Butterworth-Heinemann, Oxford, **1980**.

[70] Chaikin, P. M.; Lubensky, T. C. *Principles of Condensed Matter Physics*. Cambridge University Press, **1995**.

[71] Hansen, J.-P.; McDonald, I. *Theory of Simple Liquids*. Academic Press, Elsevier, Amsterdam, 3rd ed., **2006**.

[72] Perera, A.; Mazighi, R. Simple and complex forms of disorder in ionic liquids. *Journal of Molecular Liquids* **2015**. *210*, 243–251. Mesoscopic structure and dynamics in ionic liquids.

[73] Santos, C.; Annapureddy, H. R.; Murthy, N.; Kashyap, H.; Castner, E.; Margulis, C. Temperature-dependent structure of methyltributylammonium bis(trifluoromethylsulfonyl)amide: X ray scattering and simulations. *The Journal of Chemical Physics* **2011**. *134*, 064501.

[74] Siqueira, L.; Ribeiro, M. Charge ordering and intermediate range order in ammonium ionic liquids. *The Journal of Chemical Physics* **2011**. *135*, 204506.

[75] Annapureddy, H.; Kashyap, H.; De Biase, P.; Margulis, C. What is the origin of the prepeak in the x-ray scattering of imidazolium-based room-temperature ionic liquids? *The Journal of Physical Chemistry B* **2010**. *114*, 16838–16846. PMID: 21077649.

[76] Perera, A. Charge ordering and scattering pre-peaks in ionic liquids and alcohols. *Physical Chemistry Chemical Physics* **2017**. *19*, 1062.

[77] Perera, A. From solutions to molecular emulsions. *Pure and Applied Chemistry* **2016**. *88*, 189.

[78] Perera, A. Molecular emulsions: from charge order to domain order. *Phys. Chem. Chem. Phys.* **2017**. *19*, 28275–28285.

[79] Morawiec, A. *Indexing of Crystal Diffraction Patterns: From Crystallography Basics to Methods of Automatic Indexing*. Springer Series in Materials Science. Springer International Publishing, **2022**.

[80] Požar, M.; Lovrinčević, B.; Perera, A. The influence of charge ordering in the microscopic structure of monohydroxy alcohols. *Journal of Physics: Condensed Matter* **2024**. *36*, 265102.

[81] Soper, A. K. Computer simulation as a tool for the interpretation of total scattering data from glasses and liquids. *Molecular Simulation* **2012**. *38*, 1171–1185.

[82] Yamaguchi, T.; Hidaka, K.; Soper, A. The structure of liquid methanol revisited: a neutron diffraction experiment at -80 c and +25 c. *Molecular Physics* **1999**. *96*, 1159.

[83] Kolaříková, A.; Perera, A. Concentration fluctuation/microheterogeneity duality illustrated with aqueous 1,4-dioxane mixtures. *Journal of Chemical Theory and Computation* **2024**. *20*, 3473–3483. PMID: 38687823.

[84] Kiselev, M. A.; Lombardo, D. Structural characterization in mixed lipid membrane systems by neutron and x-ray scattering. *Biochimica et Biophysica Acta (BBA) - General Subjects* **2017**. *1861*, 3700–3717. Science for Life - Recent Advances in Biochemical and Biophysical Methods.

[85] Bunkin, N. F.; Shkirin, A. V.; Lyakhov, G. A.; Kobelev, A. V.; Penkov, N. V.; Ugraitskaya, S. V.; Fesenko, J., E. E. Droplet-like heterogeneity of aqueous tetrahydrofuran solutions at the submicrometer scale. *The Journal of Chemical Physics* **2016**. *145*, 184501.

[86] SedlÃ¡k, M.; Rak, D. On the origin of mesoscale structures in aqueous solutions of tertiary butyl alcohol: The mystery resolved. *The Journal of Physical Chemistry B* **2014**. *118*, 2726–2737. PMID: 24559045.

[87] D'Arrigo, G.; Giordano, R.; Teixeira, J. Small-angle neutron scattering studies of aqueous solutions of linear alkanediols and triols. *Langmuir* **2000**. *16*, 1553–1556.

[88] D'Arrigo, G.; Giordano, R.; Teixeira, J. Small-angle neutron scattering studies of aqueous solutions of short-chain amphiphiles. *The European Physical Journal E* **2003**. *10*, 135.

[89] D'Arrigo, G.; Giordano, R.; Teixeira, J. Temperature and concentration dependence of sans spectra of aqueous solutions of short-chain amphiphiles. *The European Physical Journal E* **2009**. *29*, 37.